may prove to be a useful complement to existing methods for determining λ.[8]

We are indebted to P. B. Allen, A. B. Pippard, and J. A. Rayne for illuminating discussions, and to N. E. Christensen for kindly supplying the one-electron potential. Financial support by the Natural Sciences and Engineering Research Council of Canada is gratefully acknowledged.

[1]A. B. Pippard, Proc. Roy. Soc. London, Ser. A 257, 165 (1960).

[2]P. L. Taylor, *A Quantum Approach to the Solid State* (Prentice-Hall, Englewood Cliffs, 1970), Chap. 5.

[3]E. Fawcett, R. Griessen, W. Joss, M. J. G. Lee, and J. M. Perz in *Electrons at the Fermi Surface*, edited by M. Springford (Cambridge Univ. Press, Cambridge, 1980), Chap. 7, and references therein.

[4]N. E. Christensen, private communication. Some details of the potential V_2 are given in N. E. Christensen and B. Feuerbacher, Phys. Rev. B 10, 2349 (1974).

[5]M. Redwood and J. Lamb, Proc. Phys. Soc., London, Sect. A 70, 136 (1957).

[6]D. Glotzel, D. Rainer, and H. R. Schober, Z. Phys. B 35, 317 (1979).

[7]C. K. Jones and J. A. Rayne, Phys. Lett. 13, 282 (1964).

[8]G. Grimvall, *The Electron-Phonon Interaction in Metals* (North-Holland, Amsterdam, 1981), Chap. 10.

Measurement of the Velocity of the Crystal-Liquid Interface in Pulsed Laser Annealing of Si

G. J. Galvin, M. O. Thompson, and J. W. Mayer
Department of Material Science, Cornell University, Ithaca, New York 14853

and

R. B. Hammond and N. Paulter
Los Alamos National Laboratories, Los Alamos, New Mexico 87544

and

P. S. Peercy
Sandia National Laboratories, Albuquerque, New Mexico 87185

(Received 13 October 1981)

The conductance of Au-doped Si single crystals was measured during irradiation with 30-nsec Q-switched ruby-laser pulses at energy densities above the Si melting threshold (~ 0.9 J/cm^2). The sample conductance is determined primarily by the thickness of the molten layer so that the solid-liquid interface velocity can be found from the current transient. The interface velocity during crystallization was found to be 2.7 ± 0.1 m/sec, in close agreement with calculated values based on a heat-flow model.

PACS numbers: 68.45.-v, 72.15.Cz, 79.20.Ds, 81.40.Ef

Pulsed laser and electron-beam annealing has been used to induce nearly perfect crystal regrowth in ion-implantation-damaged silicon. Sufficient energy can be deposited to melt a surface layer; this has led to studies of differences in the melting temperatures of amorphous and crystalline Si.[1] The diffusion coefficients of impurities in molten Si are large, $D_l \sim 10^{-4}$ cm^2/sec, so that the redistribution of implanted species occurs within the molten Si.[2] After the termination of the irradiation pulse, epitaxial regrowth occurs as the liquid-solid interface moves back toward the surface at velocities, v, calculated[3,4] to lie between 1 and 10 m/sec. The interface velocity has a critical influence on the dopant segregation and trapping ($D_l/v \cong 10^{-6}$ to 10^{-7} cm) as well as interface stability.[5,6]

Prior to this work, there had been no direct measurements of either the velocity of the liquid-solid interface or the total volume of molten Si. The duration of the melt has been determined by time-resolved reflectivity of the metallic behavior of molten Si.[7] The duration has also been estimated from the diffusion of impurities.[1,5] However, in the absence of direct confirmation of the predicted liquid-solid interface motion, a nonthermal model has also been proposed[8] in which the laser energy is transformed into highly excited carriers and the lattice itself remains relatively cold. Raman-scattering measurements[9]

support the nonthermal model by indicating a lattice temperature rise of only 300 K. However, time-of-flight measurements[10] of the temperature of evaporated Si atoms indicate a lattice temperature of between 1200 and 3000 K during pulsed laser annealing and hence support a strictly thermal model of surface melting.

We report here transient conductance measurements during Q-switched ruby-laser irradiation of single-crystal Si. The volume of molten Si and the velocity of the liquid-solid interface can be directly calculated from these measurements. The transformation of Si from a solid to a molten state at the melting temperature, T_m, leads to a thirty-fold change in resistivity ($\rho_{\text{liquid Si}} = 80$ $\mu\Omega$ cm).[11] Low-lifetime Au-doped Si was used to prevent the photogenerated free carriers from dominating the sample conductance for appreciable times after the termination of the laser pulse. As the photoconductive response decays, the sample conductance is determined primarily by the thickness of the molten layer. Because of the strong thermal gradient near the interface ($\partial T/\partial z \cong 10^6$ K/cm), the thermally generated free carriers in the solid Si contribute less than 2% to the overall conductance of a 0.5-μm molten layer. Consequently, measurement of the sample conductance provides a direct measure of the volume of molten Si. The present measurements provide direct confirmation of the thermal model.

Polished slices, 250 μm thick, were prepared from ⟨111⟩ Si doped with Au by thermal diffusion at 1300 °C to reduce the carrier lifetime. Samples, 1 cm by 1 mm, were cut and Al contacts were evaporated on both ends of the top surface, resulting in a contact-to-contact spacing of 7.7 mm. The samples were then mounted in cutout *HN* connectors, Fig. 1. Irradiation was provided by a Q-switched ruby laser ($\tau \cong 30$ nsec full width at half maximum) through a quartz tube homogenizer, evenly illuminating the entire sample, including contacts. The incident energy density was varied by neutral density filters. The equivalent circuit is shown in Fig. 1. A relatively high bias voltage (40 V) was used to avoid nonlinearities in the contact resistances. Fast capacitors were mounted near the sample to keep transients on the bias voltage to less than 1.5 V. Laser power was monitored by both a fast photodetector and an integrating detector to provide energy calibration.

Samples were irradiated with laser pulses at energy densities between 0.1 and 2.6 J/cm^2. The current transients (measured across the

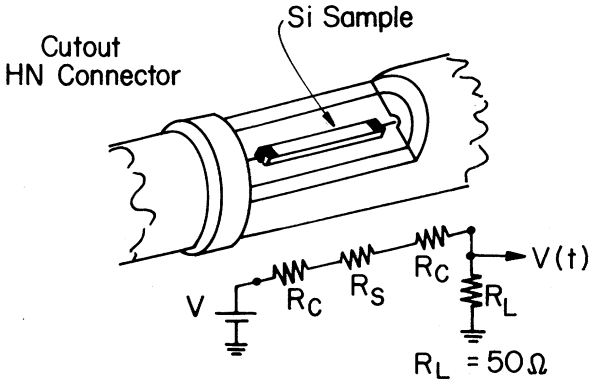

FIG. 1. Schematic drawing of the sample and holder geometry and equivalent circuit.

50-Ω load) for energy densities between 0.1 and 0.8 J/cm^2 were essentially identical, showing only the photoconductive response; a current trace at 0.35 J/cm^2 is shown in Fig. 2(a). The peak current is determined by the contact and load resistances only (total inferred contact resistance < 2.5 Ω in this sample) since the photoconductive sample resistance is essential zero. At power levels above 0.9 J/cm^2, the current transients broadened as shown in Fig. 2(a). Similar curves were obtained from other samples Au-doped at either 1200 or 1300 °C. The data were also repeatable after cycling through the power range several times. At an energy density of about 2.0 J/cm^2, the sample resistance became comparable to that of the load resistance and the curves exhibit a convex shape. The actual conductance of the sample is deconvoluted from these curves as shown in Fig. 2(b) for the 2.6-J/cm^2 case. The conductance decreases almost linearly with time over the interval of 150 to 300 nsec after the start of the laser pulse. The vertical dashed line at 135 nsec is approximately the duration of the photoconductance, based on irradiation at 0.8 J/cm^2 and below.

The conductance transients for energy densities between 1.2 and 2.6 J/cm^2 are shown in Fig. 3(a) for $t > 135$ nsec. At higher energy densities, the conductance increases and persists for longer times. The conductance can be linearly related to an apparent melt depth by geometric factors (sample width and length) and the resistivity of molten Si ($\rho_l = 80$ $\mu\Omega$ cm). Thus the curves in Fig. 3(a) also represent the thickness of the molten layer (melt depth) versus time. The velocity of the liquid-solid interface during recrystallization is given by the slope of these curves. The linear portions of the 1.9- to 2.6-J/cm^2 curves

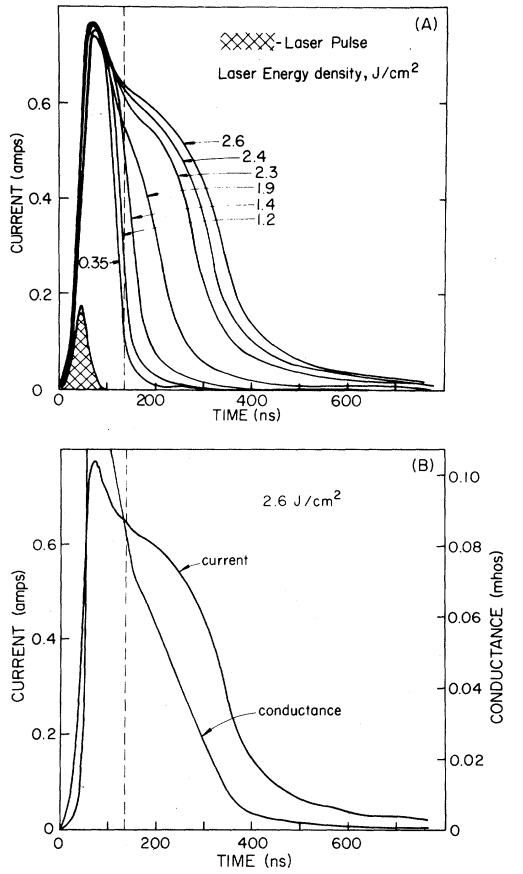

FIG. 2. (a) Current vs time for a sample irradiated with a Q-switched ruby laser at energy densities between 0.35 and 2.6 J/cm^2. The laser pulse is indicated by the cross-hatched curve. (b) Current and conductance ($R_c = 0.6\,\Omega$) for a sample irradiated with 2.6 J/cm^2. The vertical dashed line represents the duration of the photoconductance.

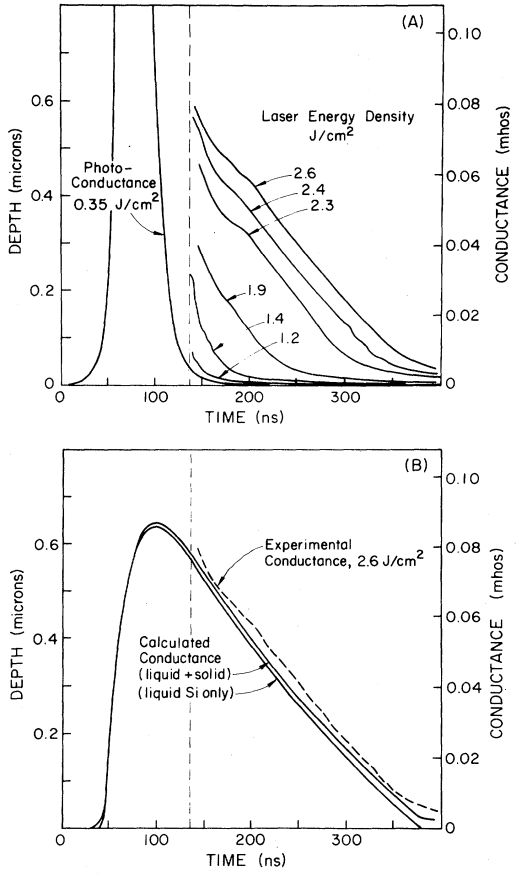

FIG. 3. (a) Conductance vs time for the data of Fig. 2(a). The depth scale is derived by assuming that the conductance is determined only by the conductivity of molten Si. (b) Calculated curves, based on a thermal heat-flow model, of the conductance of liquid and near interface solid Si (upper curve) and liquid Si only (lower curve). Dashed line is the experimentally obtained curve for 2.6 J/cm^2 ($R_c = 0.6\,\Omega$).

indicate an interface velocity of 2.7 ± 0.1 m/sec. The uncertainty in the interface velocity reflects the uncertainty in the contact resistance.

During recrystallization, the latent heat of melting liberated at the advancing interface is just balanced by heat conduction into the substrate:

$$\Delta H_c \rho v = \kappa \partial T/\partial z\,, \qquad (1)$$

where ΔH_c is the enthalpy of melting, ρ the density, and κ the thermal conductivity. Numerical calculations similar to those of Baeri *et al.*[3] and Wood and Giles[4] have been made of the conductance (excluding photoconductance) for comparison with experimental results. Included in the numerical calculations were the temperature-dependent values of thermal conductivity, specific heat, and electrical conductivity. An effective absorption length of 1.0 μm was used for solid Si to include the effects of free-carrier absorption. The value of the absorption length was chosen so that the calculated value of the melting threshold (0.8 J/cm^2) matched the experimental[12] value. Based on optical measurements[12] the discontinuous change of both the absorption length (1.0 to 0.02 μm) and the reflectivity (35% to 72%) as the surface melts was also included. The lower curve in Fig. 3(b) shows the conductance of liquid Si or melt depth versus time from these calculations for an incident power of 2.6 J/cm^2. The upper curve in Fig. 3(b) shows the apparent melt depth obtained by including the conductivity of the thermally generated carriers near the liquid-solid interface. This contribution is equivalent to a thickness of molten Si of about 6 nm.

The small difference between the two curves indicates that the apparent melt depth calculated from the measured conductance is a reasonable estimate of the actual melt depth. Furthermore, since the two calculated curves are nearly parallel, the regrowth velocity can be estimated from the slope of the total conductance. The lower curve gives an average value of $v = 2.6$ m/sec for a melt duration of 300 nsec.

The experimental procedure presented here is relatively simple, requiring only low-lifetime material and a tenfold increase in the conductivity at melting. Hence, the technique can be applied not only to crystalline and amorphous Si, but also to Ge and compound semiconductors, to obtain melt depths and liquid-solid interface velocities. The close agreement between the experimental (dashed line) and calculated conductance curves in Fig. 3(b) provides strong evidence for annealing via a purely thermal process. Although the photoconductive response prevented measurement of the advancing melt front in this work, it may be possible to observe it in even shorter-lifetime material such as amorphous Si. The direct information on the location of the liquid-solid interface, furnished by this technique, provides confirmation for our understanding of thermal aspects of the mechanisms involved in laser annealing.

This work was supported in part by the U. S. Defense Advanced Research Projects Agency through the U. S. Office of Naval Research and by the U. S. Department of Energy under Contract No. EE-AC04-76-DP00789.

[1]P. Baeri, G. Foti, J. M. Poate, and A. G. Cullis, Phys. Rev. Lett. 45, 2036 (1980).

[2]C. W. White, P. P. Pronko, S. R. Wilson, B. R. Appleton, J. Narayan, and R. T. Young, J. Appl. Phys. 50, 3261 (1979).

[3]P. Baeri, S. U. Campisano, G. Foti, and E. Rimini, J. Appl. Phys. 50, 788 (1979).

[4]R. F. Wood and G. E. Giles, Phys. Rev. B 23, 2923 (1981).

[5]A. G. Cullis, H. C. Weber, J. M. Poate, and A. L. Simons, Appl. Phys. Lett. 36, 320 (1980).

[6]J. Narayan, J. Appl. Phys. 52, 1289 (1981).

[7]D. H. Auston, J. A. Golovchenko, P. R. Smith, C. M. Surko, and T. N. C. Venkatesan, Appl. Phys. Lett. 33, 538 (1978).

[8]J. A. Van Vechten, R. Tsu, F. W. Saris, and D. Hoonhout, Phys. Lett. 74A, 417 (1979).

[9]H. W. Lo and A. Compaan, Phys. Rev. Lett. 44, 604 (1980).

[10]B. Stritzker, A. Pospieszczyk, and J. A. Tagle, Phys. Rev. Lett. 47, 356 (1981).

[11]T. E. Farber, *Theory of Liquid Metals* (Cambridge Univ. Press, Cambridge, England, 1972).

[12]P. S. Peercy, to be published.